Core-valence correlations for atoms with open shells

V. A. Dzuba and V. V. Flambaum
School of Physics, University of New South Wales, Sydney 2052, Australia
(Received 11 March 2007; published 11 May 2007)

We present an efficient method of inclusion of the core-valence correlations into the configuration interaction (CI) calculations. These correlations take place in the core area where the potential of external electrons is approximately constant. A constant potential does not change the core electron wave functions and Green's functions. Therefore, all operators describing interaction of M valence electrons and N-M core electrons [the core part of the Hartree-Fock Hamiltonian V^{N-M}, the correlation potential $\hat{\Sigma}_1(\mathbf{r},\mathbf{r}',E)$, and the screening of interaction between valence electrons by the core electrons $\hat{\Sigma}_2$] may be calculated with all M valence electrons removed. This allows one to avoid subtraction diagrams which make accurate inclusion of the core-valence correlations for $M>2$ prohibitively complicated. Then the CI Hamiltonian for M valence electrons is calculated using orbitals in complete V^N potential (the mean field produced by all electrons); $\hat{\Sigma}_1+\hat{\Sigma}_2$ are added to the CI Hamiltonian to account for the core-valence correlations. We calculate $\hat{\Sigma}_1$ and $\hat{\Sigma}_2$ using many-body perturbation theory in which dominating classes of diagrams are included in all orders. We use neutral Xe I and all positive ions up to Xe VIII as a testing ground. We found that the core electron density for all these systems is practically the same. Therefore, we use the same $\hat{\Sigma}_1$ and $\hat{\Sigma}_2$ to build the CI Hamiltonian in all these systems ($M=1,2,3,4,5,6,7,8$). Good agreement with experiment for energy levels and Landé factors is demonstrated for all cases from Xe I to Xe VIII.

DOI: 10.1103/PhysRevA.75.052504 PACS number(s): 31.25.Eb, 31.25.Jf

I. INTRODUCTION

Accurate calculations for many-electron atoms play an important role in many advanced topics of modern physics. This includes parity and time invariance violating phenomena in atoms [1], search for manifestation of possible variation of fundamental constants in astrophysical data [2], or in present-day laboratory experiments [3], improving accuracy of atomic clocks [4], study of superheavy elements (see, e.g. [5]), etc. Calculations are needed for planning of experiments and interpretation of the results.

Atoms of the most interest for the listed topics are usually found in the second part of the Periodic Table where measurements or observations are more likely to give useful information due to strong enhancement of the effects caused by interplay between relativistic and many-body effects. On the other hand, accurate treatment of relativistic and many-body effects represent a big challenge for atomic calculations. Not surprisingly, the number of methods capable of producing reliable and accurate results is very limited. The most advanced methods have been developed for atoms with one external electron above closed shells. For example, most accurate calculations of the parity nonconservation in cesium where carried out with two most advanced methods. One was the correlation potential (CP) method [6] combined with the all-order perturbation theory in screened Coulomb interaction [7] and the other was the linearized coupled cluster approach [8]. With these two methods, energy levels and transition amplitudes for alkali-metal atoms can be calculated to the accuracy of fraction of percent while hyperfine structure and parity violating amplitudes are calculated to the accuracy of 0.5–1 % [7–9].

For atoms with more than one external electron in open shells the accuracy of calculations is significantly lower. For example, the best accuracy achieved for parity non conservation (PNC) in Tl is around 3% (3% in Ref. [10] and 2.5% in Ref. [11]). Typical accuracy for energies is about 1% or worse. The main challenge is the need for accurate treatment of both core-valence and valence-valence correlations. The most commonly used methods can be divided in several main groups: (a) Many-body perturbation theory (MBPT) (see, e.g. [12]), (b) coupled cluster approach (CC) (see, e.g. [13]), (c) configuration interaction (CI) (see, e.g. [14]), and (d) multiconfiguration Dirac-Fock method (MCDF) (see, e.g. [15]). There are also combinations of these basic techniques.

All of these method have their limitations. For example, CI usually treats correlations between valence electrons very accurately but core-valence correlations are either totally neglected or only small fraction of them is included. MBPT can include more core-valence correlations, but its application to the correlations between valence electrons is limited by the fact that these correlations are often too strong to be treated perturbatively. The CC approach includes certain types of core-valence and valence-valence correlations in all orders and in principle can be formulated for any number of valence electrons. However, the equations are complicated and most of practical realization of the method deal with only one or two electrons (or an electron and a hole).

Significant progress can be achieved by combining different techniques. In 1996 we developed a method which combines the MBPT with the CI method (CI+MBPT) [16]. Here, the second-order MBPT was used to construct the effective Hamiltonian in the valence space which includes the core-valence correlations. It differs from the standard CI Hamiltonian by an extra correlation operator $\hat{\Sigma}$ which accounts for the core-valence correlations. Single-electron part of this operator is very similar to the correlation potential used for atoms with one external electron [6]. It was demonstrated that inclusion of the core-valence correlations lead to a significant improvement of the accuracy of calculations (see,

 ©2007 The American Physical Society

e.g. [16–19]). Savukov and co-workers [20] developed a version of the method which uses the hole-particle formalism. They applied the technique for a calculation of the electron structure of the noble-gas atoms [20,21].

The CI+MBPT method was successfully used for a number of atoms with two or three valence electrons [16,17,22] (or an electron and a hole [20,21]). Its extension to atoms with more electrons in open shells meets some difficulties. It turns out that convergence of the MBPT varies very much from atom to atom and strongly depends on an initial approximation. The core-valence correlations are often too large if treated in the same fashion as in our original works and their inclusion does not improve the results.

It is widely accepted that the Hartree-Fock potential is the best choice as a zero approximation for consequent use of the MBPT due to great reduction of the terms caused by exact cancellation between the potential and electron-electron Coulomb terms. However, for atoms with open shells HF procedure is not defined unambiguously. This is especially true when the CI method is to be used. Here we have freedom of how many electrons are to be included into the initial HF procedure and how many electrons are to be treated as valence electrons in the CI calculations. It was found in our previous work [23] that for a wide range of atoms the best choice is the so-called V^{N-M} approximation. These are the atoms in which valence electrons form a separate shell, defined by the same principal quantum number. For example, the ground state configuration of xenon is $[\mathrm{Pd}]5s^25p^6$. Its eight outermost electrons have $n=5$ while all other electrons have $n<5$. This means that eight outermost electrons should be treated as valence electrons and the initial HF procedure should not include them. This greatly simplifies the MBPT, improves its convergence and allows one to include higher-order correlations in the same way as it was done for atoms with one external electron.

The aim of the present work is to develop a solid theoretical background for use of the V^{N-M} potential as a starting point. In principle, this starting point is equivalent to any other choice of the initial HF potential. Indeed, the actual role of the *subtraction diagrams* in the correlation operators $\hat{\Sigma}$ is to reduce results obtained with any zero approximation to V^{N-M} results (see an explanation below). However, the technique for V^{N-M} is much simpler (no subtraction diagrams) and allows us to sum dominating chains of higher order diagrams to all orders (it is practically impossible for other choice of zero approximation). This results in a higher accuracy. Another advance of the present work is the use of a compact basis for valence states. In our previous works [22–25] we used the same basis to calculate $\hat{\Sigma}$ and to do the CI calculations. The basis was formed from the eigenstates of the $\hat{V}^{N-M}$ potential. This had an advantage of having the same single- and double-electron matrix elements for all ions of the same atom. Moving from ion to ion was easy, requiring only change the number of electrons in the CI calculations. However, convergence of the CI calculations rapidly deteriorated with growing number of electrons. When number of electrons became as large as eight, saturation of the basis was very hard to achieve unless huge computer resources were used. In present work we demonstrate that the basis states for valence electrons do not have to be eigenstates of the $\hat{V}^{N-M}$ potential. Instead, HF states calculated in the mean field of all electrons (of a neutral atom or corresponding positive ion) can be used after minor modifications. In this case we have to recalculate the CI basis when we change the number of valence electrons M. However, the gain is much larger. Since HF states are already good approximations to the wave functions of valence electrons we can limit the basis to just few states in each partial wave. Therefore, even for eight valence electrons the CI matrix is small, its calculation and diagonalization takes little time but the final results are very accurate.

We calculate energy levels and Landé g factors for neutral xenon and all its positive ions from X II to Xe VIII for illustration on how the technique works. Good agreement with experiment is demonstrated for all cases while very little computer resources are needed on every stage of the calculations.

II. CORE ELECTRON DENSITY AND POTENTIAL IN V^{N-M} AND V^N APPROXIMATIONS

The effective Hamiltonian of the CI method has the form (see, e.g. [16])

$$\hat{H}^{\mathrm{eff}} = \sum_{i=1} \hat{h}_{1i} + \sum_{i<j} \frac{e^2}{|\mathbf{r}_i - \mathbf{r}_j|}. \tag{1}$$

Summation goes over valence electrons, $\hat{h}_1(r_i)$ is the one-electron part of the Hamiltonian

$$\hat{h}_1 = c\alpha\mathbf{p} + (\beta - 1)mc^2 - \frac{Ze^2}{r} + V_{\mathrm{core}}, \tag{2}$$

α and β are the Dirac matrices, Ze is the nuclear charge, and V_{core} is the electrostatic potential created by the core electrons. Regardless of initial approximation used to calculate core and valence states, the valence electrons never contribute to V_{core} directly. They can only contribute to V_{core} via the self-consistent HF procedure or via any other potential used to represent valence electrons. If the core electrons and valence electrons belong to different shells the effect of the valence electrons on electron states in the core and thus on V_{core} can be extremely small. Indeed, in this case the overlap between density of the valence electrons and density of the core electrons is small. Therefore, the exchange interaction between the core and valence electrons, which is proportional to the overlap, is negligible in comparison with energy of the core electrons. On the other hand, the direct potential created by the valence electrons is practically constant inside the core since nearly all charge of the valence electrons is located outside the core. Constant potential corresponds to zero electric field and cannot have any effect on the wave function of the core electrons. The only effect of the constant potential V_0 is in energy shift $\delta E = V_0$. However, it does not change the single-particle wave functions and Green's functions of core electrons since the wave equation contains the difference $E - V_0$ which does not change. We may formulate this conclusion using the perturbation theory. In first order in

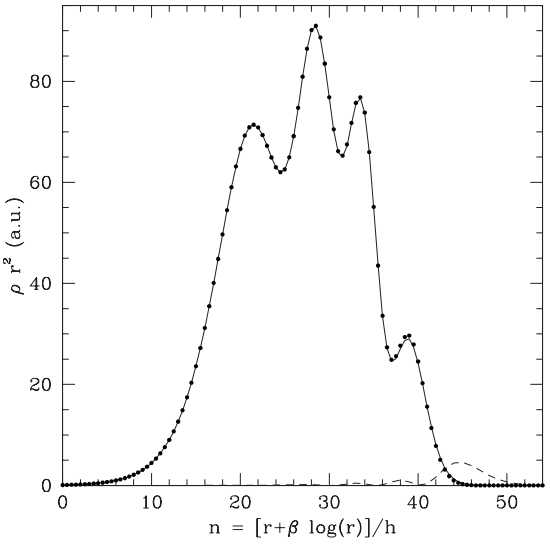

FIG. 1. Electron densities ρ (multiplied by r^2) of Xe I and Xe IX. Atomic core $(n=1,2,3,4)$ of Xe I, solid line; $5s$ and $5p$, dashed line; electron density of Xe IX, dots.

V_0 a core state a in the V^{N-M} approximation and $\tilde{a}$ in the V^N approximation are related by

$$|\tilde{a}\rangle = |a\rangle + \sum_n \frac{\langle a|V_0|n\rangle}{E_a - E_n}|n\rangle. \tag{3}$$

If the potential V_0 is constant, the matrix element $\langle a|V_0|n\rangle = V_0\langle a|n\rangle = 0$ due to the orthogonality condition. This explains why the changes of the core wave functions, density, and potential are very small.

Small overlap between the core and valence states usually takes place when these states correspond to different atomic shells defined by the principal quantum number (see, e.g. [23–25]). In the case of xenon, eight outermost electrons have principal quantum number $n=5$ (the $5s^25p^6$ ground state configuration), while all core electrons have $n<5$. Therefore, if the eight electrons are considered to be valence electrons we should expect that they have little effect on the core states. Figure 1 shows electron densities of Xe I and Xe IX calculated in the HF approximation. For the neutral Xe I electron densities of valence and core electrons are shown separately. One can see that the overlap between them is indeed very small. Therefore, it turns out that when electron density of Xe IX is calculated it practically coincides with the electron density of the core states of neutral Xe. The former is shown by dots of Fig. 1. Resolution of this figure does not allow us to see any difference between electron densities of Xe IX and the core of Xe I. This is in spite of huge difference in energies of core states of two atoms. One may argue that huge difference in energies should lead to a noticeable difference in wave functions, at least on large distances. Indeed, a wave function of an atomic electron has asymptotic defined by its energy and potential

$$\psi(r) \sim e^{-\int\sqrt{2m[E-V(r)]}dr}. \tag{4}$$

However, in the area up to the radius of the valence shell there is actually no difference in $E-V(r)$ for the core orbitals in Xe IX and Xe I since $\delta E = \langle \delta V \rangle$. The difference in asymptotic behavior appears only near the radius of the valence shell where the core electron density is extremely small.

Thus we conclude that the core electron density and potential have practically no dependence on the number of valence electrons if the valence electrons are in a different shell.

III. CORE-VALENCE CORRELATION CORRECTIONS IN THE V^N AND V^{N-M} APPROXIMATIONS

The use of the Feynman diagram technique allows us to express the core-valence correlation corrections in terms of the single-particle wave functions and Green's functions [7] (see the Appendix). Therefore, all the arguments presented above are applicable when we consider calculation of the correlation operators $\hat{\Sigma}_1$ and $\hat{\Sigma}_2$; they may be calculated using V^{N-M} basis for core electrons.

It may be instructive to clarify this conclusion using more popular Schrödinger perturbation theory where explicit summation over intermediate states is involved. The correlations between the valence and core electrons as well as the screening of the interaction between the valence electrons happen inside the area occupied by the core electrons. Let us enclose the core by a sphere with zero boundary condition for the core electrons. This allows us to reduce the core electron problem to the discrete spectrum. Let us now consider the interaction of the core electrons with external electrons using the perturbation theory. The constant potential V_0 of external electrons does not change the core electron wave functions. It also does not change the energy differences $E_n - E_m$ between the enclosed "core" states, they are shifted by the same energy V_0 (note that these enclosed states form complete basis set inside the sphere). Therefore, all the terms in the perturbation theory for the core-valence interaction (beyond the mean field which we take into account in the V^N valence orbitals) do not depend on the spectator valence electrons. This is why we can calculate all core-valence correlations using the V^{N-M} core orbitals. To avoid misunderstanding we should note that we use this picture for the explanation only, no special boundary conditions for core electrons are needed for actual calculations (it is obvious if we use the Green's function technique; all the integrals over coordinates are dominated by the core area where the correlations between the valence and core electrons actually happen). Note that below we do not neglect effects of V_0, we only treat them as a perturbation since the nondiagonal matrix elements $\langle a|V_0|n\rangle$ are small.

The effective Hamiltonian of the CI+MBPT method has the form similar to Eq. (1) but with extra terms for single and double electron parts of it. These terms, for which we use notation $\hat{\Sigma}$, describe the core-valence correlations [16]. There is a single-electron operator $\hat{\Sigma}_1$ which is added to the single-electron part $\hat{h}_1$ (2) of the CI Hamiltonian:

$$\hat{h}_1(r) \to \hat{h}_1 + \hat{\Sigma}_1. \tag{5}$$

$\hat{\Sigma}_1$ describes correlations between a particular valence electron and core electrons. It is very similar to the correlation

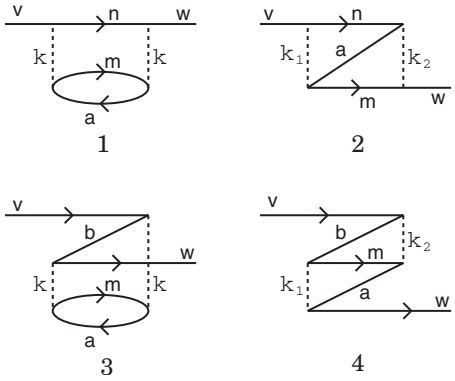

FIG. 2. Second-order diagrams for single-electron correlation operator $\hat{\Sigma}_1^{(2)}$.

potential $\hat{\Sigma}$ used for atoms with one external electron (see, e.g. [6]).

There is also a two-electron operator $\hat{\Sigma}_2$ which modifies Coulomb interaction between valence electrons:

$$\frac{e^2}{|\mathbf{r}_1-\mathbf{r}_2|} \to \frac{e^2}{|\mathbf{r}_1-\mathbf{r}_2|} + \hat{\Sigma}_2. \tag{6}$$

Physical interpretation of $\hat{\Sigma}_2$ is the screening of Coulomb interaction between valence electrons by core electrons.

When number of valence electrons is greater than 2 there is also a three-body operator $\hat{\Sigma}_3$ [16] and higher-order many-body operators $\hat{\Sigma}_4$, $\hat{\Sigma}_5$, etc. However, they are usually very small and we will not consider them in the present work.

The full set of diagrams for $\hat{\Sigma}_1$ and $\hat{\Sigma}_2$ in the second order of MBPT is presented on Figs. 2–5. It contains the so-called *subtraction* diagrams which are proportional to $V_{\text{core}}-V^{\text{HF}}$, where V_{core} is the potential of the core electrons as in the effective CI Hamiltonian (1), V^{HF} is the potential in which states of the core were calculated. Note that subtraction diagrams vanish in the V^{N-M} approximation: $V_{\text{core}}=V^{\text{HF}}$.

The origin of the subtraction diagrams is clear from the definition of the perturbation (residual interaction) operator $U=H_{\text{exact}}-H_0$ where H_{exact} is the exact Hamiltonian and H_0 is the zero approximation Hamiltonian. If the field of external electrons is included in H_0 it produces additional contributions which we call the subtraction diagrams. Thus the potential V_0 appears with positive sign in the mean field (and core wave functions), and with negative sign in the residual interaction (and subtraction diagrams). If we calculate all correlations exactly, to all orders, V_0 must disappear in the final result. In any finite order of the many-body perturbation

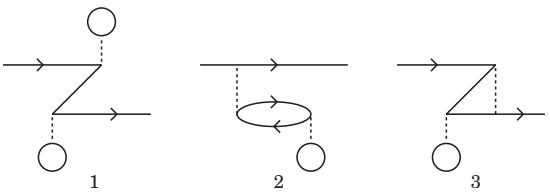

FIG. 3. Subtraction diagrams for $\hat{\Sigma}_1^{(2)}$.

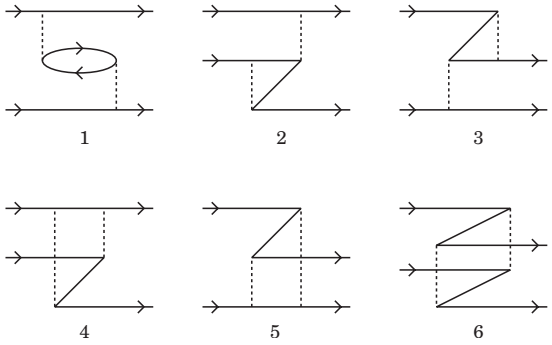

FIG. 4. Second-order diagrams for double-electron correlation operator $\hat{\Sigma}_2^{(2)}$.

theory there are only partial cancellations; lower orders of expansion in V_0 are canceled out. Thus the role of the subtraction diagrams is to cancel the potential of spectator valence electrons acting on the core electrons (effect of valence electrons on the core lines of the diagrams). In other words, the subtraction diagrams guarantee that in any given order of expansion in V_0 the operators $\hat{\Sigma}_1$ and $\hat{\Sigma}_2$ are reduced to the results of V^{N-M} approximation. Therefore, if the nondiagonal matrix elements of V_0 are small the V^{N-M} approximation is the best zero approximation since the calculations are much simpler (no subtraction diagrams).

It is easy to see all these cancellations of V_0 explicitly, order by order in V_0. Here one should remember that change of the valence electron energies due to change of the core Hartree-Fock potential (which formally has the first order in the Coulomb interaction) is actually canceled by the second order subtraction diagrams; contribution of V_0 into the core wave functions in the second order diagrams is canceled by the third order subtraction diagrams, etc.

IV. HIGHER ORDER TERMS IN $\hat{\Sigma}$

We have seen above that if the electrostatic potential V_0 created by valence electrons is nearly constant inside the core then the V^{N-M} approximation is equivalent to the $V^{N-M}+V_0$ approximation, where V_0 can have contributions from all M valence electrons, or any fraction on them or it can be just a model potential. The only condition is that V_0 is nearly constant inside the core. This means that without any compromise on accuracy we can do the calculation in the V^{N-M} approximation which is technically more simple. Another advantage of using V^{N-M} is that we have the same effective

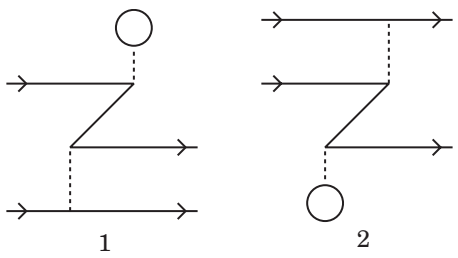

FIG. 5. Subtraction diagrams for $\hat{\Sigma}_2^{(2)}$.

TABLE I. Removal energies of lowest states of Xe VIII (cm^{-1}) in different approximations; comparison with experiment.

State	HF	$\hat{\Sigma}^{(2)a}$	$\hat{\Sigma}^{(\infty)b}$	Expt.[26]
$5s_{1/2}$	839 764	858 722	854 842	854 755
$5p_{1/2}$	725 342	741 343	738 280	738 288
$5p_{3/2}$	707 377	722 378	719 550	719 703
$5d_{3/2}$	536 494	546 174	544 092	544 867
$5d_{5/2}$	533 632	543 150	541 096	541 939
$4f_{5/2}$	572 050	590 725	587 324	589 594
$4f_{7/2}$	571 684	590 056	586 717	589 044

[a]Solving Eq. (7) with the second-order correlation potential $\hat{\Sigma}$.
[b]Solving Eq. (7) with the all-order correlation potential $\hat{\Sigma}$.

Hamiltonian for any number of valence electrons from 1 to M. Therefore we can do the calculations in a very similar way for all corresponding ions as well as for a neutral atom.

Eliminating subtracting diagrams in the V^{N-M} approximation makes $\hat{\Sigma}_1$ practically identical to the correlation potential $\hat{\Sigma}$ used for atoms with one external electron. Therefore, we can try to improve the accuracy of calculations by including important higher order terms into $\hat{\Sigma}_1$ the same way as it was done in a number of calculations for alkali atoms (see, e.g. [7,9]). We include two dominating classes of higher order diagrams into calculation of $\hat{\Sigma}_1$. One is screening of the Coulomb interaction between valence and core electrons by other core electrons. Another is interaction between an electron excited from the core and a hole in the core created by this excitation. Both classes of diagrams are included in all orders (see, e.g. [7,9] for details).

We use notation $\hat{\Sigma}_1^{(\infty)}$ for the all-order $\hat{\Sigma}$ operator as compared to $\hat{\Sigma}_1^{(2)}$ for the second-order operator. The effect of inclusion of second and higher order correlations can be illustrated by calculating of the energy levels of Xe VIII. This ion has only one valence electron and calculations for it can be done the same way as for other single-valence electron atoms (see, e.g. [7]). Instead of diagonalizing the CI matrix we solve HF-like equations for valence electrons in coordinate space, with $\hat{\Sigma}_1$ included in it:

$$(h_1 + \hat{\Sigma}_1 - \epsilon)\psi = 0. \tag{7}$$

Here single-electron Hamiltonian h_1 is given by Eq. (2) while $\hat{\Sigma}_1$ can be either $\hat{\Sigma}_1^{(2)}$ or $\hat{\Sigma}_1^{(\infty)}$. If no $\hat{\Sigma}_1$ is included then Eq. (7) gives HF energies and wave functions.

The results of calculations are presented in Table I and compared with experiment. One can see systematic significant improvement of the results when first $\hat{\Sigma}_1^{(2)}$ and then $\hat{\Sigma}_1^{(\infty)}$ are included.

We are now going to use the same $\hat{\Sigma}_1^{(\infty)}$ operator for all ions from Xe VII to Xe II and for neutral xenon. For all these ions which have more than one valence electrons the $\hat{\Sigma}_2$ operator should also be included. In the V^{N-M} approximation the $\hat{\Sigma}_2$ term is given by diagrams on Fig. 4, and no subtraction diagrams are needed. To include higher-order correlations into $\hat{\Sigma}_2$ we use screening factors the same way as we do this for the exchange diagrams of $\hat{\Sigma}_1$ (Figs. 2.2 and 2.4) (see, e.g. [7]). To explain how screening factors are found and used we need to go into more details on how the all-order correlation operator $\hat{\Sigma}_1^{(\infty)}$ is calculated. We use Feynman diagram technique to calculate *direct* diagrams (Figs. 2.1 and 3). It allows us to include an infinite chain of screening diagrams in all orders [7]. Application of the Feynman diagram technique to *exchange* diagrams (Figs. 2.2 and 4) is much more complicated [9]. On the other hand, these diagrams are usually an order of magnitude smaller than *direct* diagrams. Therefore it makes sense to use an approximate method by introducing *screening factors*. We assume that screening of Coulomb interaction between core and valence electrons depends only on multipolarity k of Coulomb interaction. Screening factors f_k are calculated as ratios of partial contributions to $\hat{\Sigma}_1$:

$$f_k = \langle \hat{\Sigma}_k^{(\infty)} \rangle \Big/ \langle \hat{\Sigma}_k^{(2)} \rangle, \tag{8}$$

where only *direct* diagrams are included in $\hat{\Sigma}_k^{(2)}$ and $\hat{\Sigma}_k^{(\infty)}$ and only screening of Coulomb interaction but no hole particle interaction is included in $\hat{\Sigma}_k^{(\infty)}$. The values of f_k found from calculations for alkali-metal atoms are

$$f_0 = 0.72, \quad f_1 = 0.62, \quad f_2 = 0.83,$$

$$f_3 = 0.89, \quad f_4 = 0.94, \quad f_5 = 1.00, \quad \text{etc.} \tag{9}$$

The values of f_k change very little from atom to atom and the values presented above can be used for xenon. This is supported by the results obtained for Xe VIII (see Table I).

The effect of $\hat{\Sigma}_2$ on atomic energies is much smaller than those of $\hat{\Sigma}_1$. Therefore, we can also treat higher-order correlations in $\hat{\Sigma}_2$ in an approximate way, via screening factors, as we do this for exchange part of $\hat{\Sigma}_1$. We replace every Coulomb integral Q_k on all diagrams on Fig. 4 except diagram Fig. 4.1 by its screened values $f_k Q_k$ where screened factors f_k are taken as in Eq. (9). For the diagram Fig. 4.1 only one of the Coulomb integrals is replaced by its screened value. This is because this diagram can generate only one infinite chain

TABLE II. Basis states of valence electrons used in the CI calculations, their total number (N) for each atom or ion, and HF configurations in which they were calculated.

Atom	N	Basis states	Configurations	
Xe I	15	$5s,6s,7s,5p,6p,7p,5d,6d,4f$	$5s^25p^6$,	$5s^25p^5nl$
Xe II	10	$5s,6s,5p,6p,5d,4f$	$5s^25p^5$,	$5s^25p^4nl$
Xe III	8	$5s,6s,5p,6p,5d$	$5s^25p^4$,	$5s^25p^3nl$
Xe IV	10	$5s,6s,5p,6p,5d,4f$	$5s^25p^3$,	$5s^25p^2nl$
Xe V	8	$5s,6s,5p,6p,5d$	$5s^25p^2$,	$5s^25pnl$
Xe VI	8	$5s,6s,5p,6p,5d$	$5s^25p$,	$5s^2nl$
Xe VII	8	$5s,6s,5p,5d$	$5s^2$,	$5snl$

TABLE III. Ground state removal energy (a.u.), excitation energies (cm^{-1}), and g factors of lowest states of Xe in different approximations.

State		J	CI	$\hat{\Sigma}_1^{(2)a}$	$\hat{\Sigma}_1^{(2)a}$ and $\hat{\Sigma}_2^{(2)b}$	$\hat{\Sigma}_1^{(\infty)c}$	$\hat{\Sigma}_1^{(\infty)c}$ and $\hat{\Sigma}_2^{(2)b}$	$\hat{\Sigma}^{(\infty)d}$		Expt.		Δ^e
			E	E	E	E	E	E	g	E	g	
$5s^25p^6$	^1S	0	−15.21	−15.76	−15.69	−15.53	−15.48	−15.49		−15.61		
$5s^25p^56s$	$^2[3/2]^\circ$	2	62 710	70 595	68 587	68 289	66 310	67 040	1.4994	67 068	1.500 95	28
		1	64 013	71 916	69 873	69 594	67 573	68 319	1.2157	68 045	1.205 5	−274
$5s^25p^56s$	$^2[1/2]^\circ$	0	71 616	80 192	78 425	77 568	75 824	76 480	0	76 197		−283
		1	72 896	81 586	79 764	78 925	77 120	77 799	1.3160	77 185	1.321	−614
$5s^25p^56p$	$^2[1/2]$	1	72 707	81 332	79 318	78 519	76 533	77 283	1.8559	77 269	1.852	−14
		0	76 219	84 202	82 183	81 602	79 607	80 350	0.0000	80 119		−231
$5s^25p^56p$	$^2[5/2]$	2	73 810	82 369	80 304	79 587	77 545	78 307	1.1005	78 120	1.111 03	−187
		3	74 045	82 627	80 568	79 837	77 802	78 564	1.3333	78 403	1.336	−161
$5s^25p^56p$	$^2[3/2]$	1	74 755	83 339	81 261	80 549	78 496	79 260	1.0232	78 956	1.023 48	−304
		2	74 964	83 540	81 466	80 755	78 705	79 468	1.3913	79 212	1.383 6	−256
$5s^25p^55d$	$^2[1/2]^\circ$	0	76 068	84 821	82 949	82 082	80 235	80 919	0	79 771		−1148
		1	76 259	84 946	83 067	82 221	80 367	81 054	1.3786	79 987	1.395	−1067
$5s^25p^55d$	$^2[7/2]^\circ$	4	76 425	84 622	82 869	81 997	80 257	80 900	1.2500	80 197	1.250 6	−703
		3	77 283	85 513	83 764	82 877	81 141	81 783	1.0762	80 970	1.074 9	−813
$5s^25p^55d$	$^2[3/2]^\circ$	2	76 370	84 667	82 973	82 001	80 323	80 947	1.3775	80 323	1.375 0	−624
		1	80 595	89 175	86 989	86 445	84 279	85 087	0.9900	83 890		−1197
$5s^25p^55d$	$^2[5/2]^\circ$	2	78 310	86 627	84 853	83 959	82 199	82 846	0.9419	81 926		−920
		3	78 626	86 996	85 209	84 306	82 531	83 184	1.2179	82 430		−754
$5s^25p^57s$	$^2[3/2]^\circ$	2	80 504	89 101	86 967	86 367	84 254	85 042	1.4910	85 189		147
		1	81 064	89 742	87 648	86 951	84 880	85 655	0.9759	85 440		−215
$5s^25p^57p$	$^2[1/2]$	1	83 048	91 935	89 859	89 051	87 001	87 773	1.7930	87 927	1.727 2	154
		0	84 221	92 910	90 834	90 110	88 057	88 825	0	88 842		17
$5s^25p^57p$	$^2[5/2]$	2	83 464	92 252	90 160	89 397	87 330	88 104	1.1107	88 352	1.127 6	248
		3	83 558	92 350	90 262	89 494	87 429	88 204	1.3333	88 469	1.330	265
$5s^25p^56p$	$^2[3/2]$	1	83 700	92 521	90 429	89 662	87 594	88 369	1.0216	88 379	0.792 5	10
		2	84 883	94 445	92 365	91 398	89 352	90 122	1.1497	89 162	1.190	−960
$5s^25p^56d$	$^2[1/2]^\circ$	0	83 637	92 398	90 367	89 562	87 557	88 309	0	88 491		182
		1	83 728	92 489	90 466	89 654	87 658	88 405	1.3430	88 550		145
$5s^25p^57p$	$^2[3/2]$	2	83 832	92 610	90 519	89 759	87 693	88 466	1.3843	88 687	1.352 0	221
		1	84 392	94 128	92 055	90 956	88 909	89 680	0.6345	88 745	0.903 9	−935
$5s^25p^56d$	$^2[3/2]^\circ$	2	83 947	92 702	90 695	89 870	87 892	88 632	1.3165	88 708		76
		1	86 666	95 327	93 442	92 542	90 699	91 378	0.6980	90 032		−1346
$5s^25p^56d$	$^2[7/2]^\circ$	4	84 071	92 767	90 743	89 952	87 956	88 701	1.2500	88 912		211
		3	84 273	92 937	90 939	90 134	88 167	88 900	1.0926	89 025		125
$5s^25p^56d$	$^2[5/2]^\circ$	2	84 610	93 238	91 272	90 449	88 514	89 232	0.9548	89 243		11
		3	84 900	93 476	91 533	90 700	88 790	89 496	1.2085	89 535		39

[a]Second-order single-electron correlation operator (CO) $\hat{\Sigma}$ is included.

[b]Second-order double-electron CO $\hat{\Sigma}$ is included.

[c]All-order single-electron CO $\hat{\Sigma}$ is included.

[d]All-order $\hat{\Sigma}_1$ and $\hat{\Sigma}_2$ are included.

[e]Difference between experiment and best calculations for the energies.

of loops representing screening. Therefore, screening should by included only once. This is very similar to the all-order treatment of the direct diagram for $\hat{\Sigma}_1$ (Figs. 2.1 and 2.3). If this diagram is expressed in terms of screened Coulomb interaction, only one of two Coulomb integrals should be replaced by a screened one (see [7,9] for details).

TABLE IV. Ground state removal energy (a.u.), excitation energies (cm^{-1}), and g factors of lowest states of Xe VII; comparison with experiment.

State		J	Expt. [26] E	Calculations E	g	Δ^a
$5s^2$	^1S	0	−7.26	−7.27		
$5s5p$	$^3P^\circ$	0	96 141	94 889	0	1 252
		1	100 451	99 394	1.4846	1 057
		2	113 676	112 598	1.5000	1 078
$5s5p$	$^1P^\circ$	1	143 259	146 337	1.0153	−3 078
$5p^2$	^3P	0	223 673	224 343	0	−670
		1	234 685	235 008	1.5000	−323
		2	251 853	252 607	1.3027	−754
$5p^2$	^1D	2	236 100	237 129	1.1962	−1 029
$5p^2$	^1S	0	273 208	281 328	0	−8 120
$5s5d$	^3D	1	287 772	291 855	0.5000	−4 083
		2	288 712	292 896	1.1663	−4 184
		3	290 340	294 591	1.3333	−4 251
$5s5d$	^1D	2	307 542	317 647	1.0015	−10 105
$5s6s$	^3S	1	354 833	358 686	2.0000	−3 853
$5s6s$	^1S	0	361 671	364 853	0	−3 182
$5p5d$	$^3F^\circ$	2	393 792	398 186	0.7405	−4 394
		3	401 413	406 187	1.0990	−4 774
		4	412 567	417 863	1.2500	−5 296

[a] $\Delta = E(\text{expt}) - E(\text{calc})$.

TABLE V. Ground state removal energy (a.u.), excitation energies (cm^{-1}), and g factors of lowest states of Xe VI; comparison with experiment.

State		J	Expt. [26] E	Calculations E	g	Δ^a
$5s^25p$	$^2P^\circ$	1/2	−9.71	−9.72	0.6667	
		3/2	15 599	15 590	1.3333	9
$5s5p^2$	^4P	1/2	92 586	90 191	2.6301	2395
		3/2	100 378	97 787	1.7247	2591
		5/2	107 205	105 036	1.5629	2169
$5s5p^2$	^2D	3/2	124 870	125 900	0.8243	−1030
		5/2	129 230	129 897	1.2366	−667
$5s5p^2$	^2P	1/2	141 837	145 429	1.1878	−3592
		3/2	159 112	162 903	1.3119	−3791
$5s5p^2$	^2S	1/2	157 996	161 647	1.5155	−3651
$5s^25d$	^2D	3/2	180 250	186 188	0.8058	−5938
		5/2	182 308	188 093	1.2004	−5785
$5s^26s$	^2S	1/2	223 478	224 641	1.9998	−1163
$5p^3$		3/2	232 586	232 997	1.3377	−411

[a] $\Delta = E(\text{expt}) - E(\text{calc})$.

V. BASIS

There are two single-electron basis sets in this problem. One is used to calculate $\hat{\Sigma}$ and the other is used to construct many-electron states of valence electrons for the CI calculations.

In principle, it is possible to use the same basis for both purposes and we did so in many of our earlier calculations [17,22–25]. The most convenient choice for the basis is the basis consisting of single-electron states calculated in the V^{N-M} potential. We use the B-spline technique to calculate the basis. Lower and upper component of each basis set is expressed as linear combination of 40 B-splines in the cavity of radius of $40a_B$. Expansion coefficients are found from the condition that the basis states are the eigenstates of HF Hamiltonian (2) with the V^{N-M} potential. The advantages of this approach are many: Core and valence states are orthogonal automatically; the basis is reasonably complete and does not depend on the number of valence electrons. The latter means in particular that if we want to change the number of valence electrons (e.g., to do the calculation for another ion) we do not have to recalculate single and double electron matrix elements. The shortcoming of this approach is rapid increase of the size of the CI matrix with the number of valence electrons. Indeed, a typical number of single-electrons basis states needed to get saturation of the basis is around 100. The number of ways valence electrons can be distributed over these 100 states grows very fast with the number of valence electrons. For eight electrons like for Xe I the matrix reaches unmanageable size, even when some configuration selection technique is used.

In the present work we use the basis described above only for calculation of $\hat{\Sigma}$. For the CI calculations we use a very compact basis of HF states of corresponding ion or neutral atom. For example, we perform HF calculations for neutral Xe I in its ground state $[\text{Pd}]5s^25p^6$ in the V^N approximation and then use the $5s$ and $5p$ states as the basis states for the CI calculations for Xe I in the V^{N-8} approximation. Other basis states like $6s$, $6p$, etc. are obtained by removing one $5p$ electron from the atom and calculating these states in the frozen field of remaining electrons. The states obtained this way are not orthogonal to the core which corresponds to the V^{N-8} potential. In the relativistic case the basis states for valence electrons must also be orthogonal to the negative energy states. Both conditions (orthogonality to the core and to the negative energy states) have been achieved in the present work by projecting a basis state on the B-spline states above the core:

$$|v\rangle \to |v'\rangle = \sum_i |i\rangle\langle i|v\rangle. \tag{10}$$

Here summation goes over states above the core. Functions $|v'\rangle$ are more suitable for the CI calculations than states $|v\rangle$ because they do not have admixture of the core and negative energy states. The problem of excluding core and negative energy states from the basis of valence electrons in relativistic calculations have been studied in detail in Refs. [27–29].

If more than one state of particular symmetry is included into the basis (like, e.g., the $6p$ and $7p$ states for Xe I) they also need to be orthogonalized to each other.

TABLE VI. Ground state removal energy (a.u.), excitation energies (cm^{-1}), and g factors of lowest states of Xe V; comparison with experiment.

State		J	Expt. [26] E	Calculations E	g	Δ^a
$5s^25p^2$	^3P	0	−11.7	−11.72		
		1	9 292	8 969	1.5000	323
		2	14 127	14 643	1.3744	−516
$5s^25p^2$	^1D	2	28 412	30 169	1.1256	−1757
$5s^25p^2$	^1S	0	44 470	47 061	0	−2591
$5s5p^3$	$^5S^\circ$	2	92 183	88 033	1.9744	4150
$5s5p^3$	$^3D^\circ$	1	115 286	115 554	0.6192	−268
		2	116 097	116 202	1.2256	−105
		3	119 919	120 152	1.3329	−233
$5s5p^3$	$^3P^\circ$	0	133 408	134 320	0	−912
		1	134 575	135 493	1.4078	−918
		2	134 703	135 579	1.3152	−876
$5s5p^3$	$^1D^\circ$	2	145 807	147 030	1.1261	−1223
$5s5p^3$	$^3S^\circ$	1	155 518	160 672	1.7362	−5154
$5s^25p5d$	$^3F^\circ$	2	156 507	159 419	0.7036	−2912
		3	160 630	163 534	1.0901	−2904
		4	169 799	172 418	1.2500	−2619
$5s5p^3$	$^1P^\circ$	1	169 673	175 704	1.1706	−6031

[a] $\Delta = E(\text{expt}) - E(\text{calc})$.

Full list of valence states for xenon and its ions used in the calculations are presented in Table II. The first column shows an atom or ion, the second column gives the total number of valence basis states, then states are listed together with the configurations in which they were calculated. Note that every state with $l > 0$ consists of two functions, e.g., $6p$ stands for $6p_{1/2}$ and $6p_{3/2}$, etc. Note also that the number of basis states is always small, much smaller than about 100 needed with the B-spline basis. This greatly outweighs the inconvenience of recalculating the basis for every ion or atom.

VI. CALCULATIONS FOR XENON AND ITS IONS

In this section we present calculations for xenon and its ions. The whole calculation scheme consists of the following steps (we use Xe I as an example).

(1) HF for Xe IX; V^{N-8} potential is obtained.
(2) Calculation of B-spline states in the V^{N-8} potential.
(3) Calculation of $\hat{\Sigma}_1$.
(4) HF for Xe I; the $5s$ and $5p$ basis states are obtained.
(5) Calculation of valence basis states.
(6) Calculation of single and double-electron matrix elements, including matrix elements of $\hat{\Sigma}_2$.
(7) Calculation and diagonalization of the CI matrix.

At first glance this scheme does not look very simple. However, none of the steps listed above are very time consuming or require large computer power. The most time consuming step is calculation of $\hat{\Sigma}$ [$\hat{\Sigma}_1$ in step (3) and $\hat{\Sigma}_2$ in step (6)]. An efficient way of calculating both $\hat{\Sigma}_1$ and $\hat{\Sigma}_2$ is presented in the Appendix. The time scale to obtain all results presented in this section while using a PC or a laptop is one day.

TABLE VII. Ground state removal energy (a.u.), excitation energies (cm^{-1}), and g factors of lowest states of Xe IV.

State		J	Expt. [26] E	Calculations E	g	Δ^a
$5s^25p^3$	$^4S^\circ$	3/2	−13.2	−13.27	1.8987	
$5s^25p^3$	$^2D^\circ$	3/2	13 267	14 619	0.9778	−1352
		5/2	17 511	18 938	1.2000	−1427
$5s^25p^3$	$^2P^\circ$	1/2	28 036	30 149	0.6667	−2113
		3/2	35 650	37 446	1.2569	−1796
$5s5p^4$	^4P	5/2	99 664	99 466	1.5814	198
		3/2	106 923	106 710	1.7055	213
		1/2	109 254	109 169	2.6286	85
$5s5p^4$	^2D	3/2	121 929	124 529	0.8925	−2600
		5/2	125 475	128 117	1.2153	−2642
$5s^25p^25d$	^2P	3/2	133 027	135 880	0.8912	−2853
		1/2	136 796	139 997	0.7788	−3201
$5s^25p^25d$	^4F	3/2	134 981	137 617	0.8501	−2636
		5/2	136 496	139 103	1.1064	−2607
		7/2	141 625	144 013	1.2649	−2388
		9/2	145 991	148 958	1.3088	−2967
$5s^25p^25d$	^2F	5/2	141 824	145 598	0.9889	−3774
		7/2	145 011	148 526	1.2658	−3515
$5s^25p^25d$	^4D	1/2	145 106	147 933	0.4037	−2827
		3/2	146 207	148 762	1.1487	−2555
		5/2	148 685	151 840	1.1799	−3155
		7/2	155 864	159 785	1.2361	−3921
$5s5p^4$	^2S	1/2	150 737	154 437	1.5219	−3700
$5s^25p^26s$	^4P	1/2	157 205	161 777	2.3294	−4572
		3/2	165 280	167 775	1.6017	−2495
		5/2	170 490	174 875	1.4873	−4385
$5s^25p^25d$	^4P	5/2	159 643	165 187	1.5539	−5544
		3/2	161 435	169 550	1.6737	−8115
		1/2	162 867	169 085	2.4382	−6218

[a] $\Delta = E(\text{expt}) - E(\text{calc})$.

Results for neutral xenon are presented in Table III while results for six positive ions from Xe VII to Xe II are presented in Tables IV–IX. For neutral xenon (Table III) we study in detail the role of core-valence correlations by including them in different approximations. The basis for valence states is kept the same in all cases (see previous section for the description of the basis). The approximations are as follows.

(1) First, we present the results of the standard CI method, with no core-valence correlations (the "CI" column of Table III). Accuracy for the energies as compared to experimental values are not very good. However, the difference does not exceed 10% which is sufficiently good for many applica-

TABLE VIII. Ground state removal energy (a.u.), excitation energies (cm^{-1}), and g factors of lowest states of Xe III.

State		J	Expt. [26] E	Expt. [26] g	Calculations E	Calculations g	Calculations Δ[a]	Calculations $E(N-1)$
$5s^25p^4$	^3P	2	−14.38		−14.36	1.4523		−14.38
		0	8 130		8 313	0	−183	8 319
		1	9 794		9 638	1.5000	156	9 528
$5s^25p^4$	^1D	2	17 099		19 086	1.0477	−1987	17 879
$5s^25p^4$	^1S	0	36 103		37 280	0	−1177	37 392
$5s5p^5$	$^3P^\circ$	2	98 262		98 847	1.4986	−585	98 729
		1	103 568		104 334	1.4553	−766	104 369
		0	108 334		108 562	0	−228	109 016
$5s^25p^35d$	$^5D^\circ$	3	111 605		110 836	1.4702	769	113 883
		2	111 856		111 066	1.4623	790	114 075
		4	112 272		111 366	1.4813	906	114 347
		1	112 450		111 506	1.4882	944	114 360
		0	112 694		112 142	0	552	114 544
$5s^25p^35d$	$^3D^\circ$	2	117 240		118 575	1.8400	−1335	122 839
		3	121 230		122 482	1.3114	−1252	126 365
		1	121 923		123 251	0.6428	−1328	127 257
$5s^25p^35d$	$^1P^\circ$	1	119 026		120 856	1.0670	−1830	122 930
$5s^25p^36s$	$^5S^\circ$	2	121 476	1.95	119 002	1.1889	2474	125 150
$5s^25p^35d$	$^3F^\circ$	2	124 691		127 328	0.8030	−2637	130 640
		3	126 120		129 045	1.0994	−2925	132 337
		4	130 174		133 970	1.1386	−3796	138 195
$5s^25p^36s$	$^3S^\circ$	1	125 617	1.77	124 152	1.7102	1465	132 504
$5s^25p^35d$	$^3G^\circ$	4	127 782		131 307	1.1977	−3525	134 519
		3	128 349		132 922	0.8245	−4573	137 183
		5	132 160		136 422	1.2000	−4262	140 435

[a] $\Delta = E(\text{expt}) - E(\text{calc})$.

tions. This is in spite of the fact that calculations for neutral xenon were done with atomic core corresponding to highly ionized Xe IX. This is another confirmation that change in the core potential V_{core} from Xe I to Xe IX is very small.

(2) Second-order $\hat{\Sigma}_1^{(2)}$ is added to the effective Hamiltonian (the "$\hat{\Sigma}_1^{(2)}$" column of Table III). The results are significantly closer to the experiment but the correction is too large. This is similar to what usually takes place with the second-order correlation correction for atoms with one external electron.

(3) Second-order $\hat{\Sigma}_2^{(2)}$ is also added (the "$\hat{\Sigma}_1^{(2)}$ and $\hat{\Sigma}_2^{(2)}$" column). As one can see $\hat{\Sigma}_2^{(2)}$ acts in a direction opposite to $\hat{\Sigma}_1^{(2)}$ and the results are even closer to the experiment.

(4) Higher orders are included in $\hat{\Sigma}_1$ while $\hat{\Sigma}_2$ is not included at all (the "$\hat{\Sigma}_1^{(\infty)}$" column). The effect of higher orders in $\hat{\Sigma}_1$ is numerically close to the effect of $\hat{\Sigma}_2$ as is evident from the comparison with previous column. This coincidence is accidental.

(5) Higher orders are included in $\hat{\Sigma}_1$ while $\hat{\Sigma}_2$ is included in second order (the "$\hat{\Sigma}_1^{(\infty)}$ and $\hat{\Sigma}_2^{(2)}$" column). The results are improved but for many states the correction is too large.

(6) Higher orders are included in both $\hat{\Sigma}_1$ and $\hat{\Sigma}_2$ (the "$\hat{\Sigma}^{(\infty)}$" column). This is the most complete calculation we have in the present work. Here we also included calculated values of Landé's g factors. The g factors are very useful for identification of the states, especially for atoms with dense spectrum where calculations do not always reproduce the correct order of the levels.

The last column of Table III presents the difference between experimental and calculated energies where calculated energies correspond to the most complete calculation ($\hat{\Sigma}^{(\infty)}$): $\Delta = E_{\text{expt}} - E_{\text{calc}}$. This difference does not exceed 2% and should mostly be attributed to incompleteness of the basis. Indeed, it is hard to expect that the basis consisting of only 15 single-electron states (from one to three in each partial wave from $l=0$ to $l=3$) to be complete. Test calculations show that adding more states to the basis do have some effect on the energies of the states. The effect is larger for higher states. For example, it is hard to expect any reasonable accuracy for the states of the $5s^25p^56d$ configuration without having the $6d$ state in the basis. But adding the $6d$ state to the basis also have some effect on the lower

TABLE IX. Ground state removal energy (a.u.), excitation energies (cm^{-1}), and g factors of lowest states of Xe II.

			Expt. [26]		Calculations		
State		J	E	g	E	g	Δ[a]
$5s^25p^5$	$^2P^\circ$	3/2	−15.16		−15.09	1.3333	
		1/2	10 537		10 763	0.6667	−226
$5s5p^6$	^2S	1/2	90 874	2.02	91 700	2.0423	−826
$5s^25p^46s$	[2]	5/2	93 068	1.56	91 729	1.5639	1339
		3/2	95 064	1.38	94 188	1.4084	876
$5s^25p^45d$	[2]	5/2	95 397	1.36	95 802	1.3473	−405
		3/2	96 033	1.18	96 534	1.1847	−501
$5s^25p^45d$	[3]	7/2	95 438	1.42	95 783	1.3940	−345
		5/2	106 475		108 559	1.0537	−2084
$5s^25p^45d$	[1]	1/2	96 858	0.50	97 388	0.5457	−530
		3/2	105 313	1.15	107 286	1.0869	−1973
$5s^25p^45d$	[4]	9/2	99 405	1.31	100 848	1.3093	−1443
		7/2	101 536	1.11	103 581	1.1524	−2045
$5s^25p^46s$	[0]	1/2	101 157	2.43	100 700	2.3677	457
$5s^25p^46s$	[1]	3/2	102 799	1.59	101 988	1.5811	811
		1/2	106 906	1.79	108 148	1.9490	−1242
$5s^25p^45d$	[1]	1/2	104 250	0.56	104 264	0.6408	−14
		3/2	107 904	1.20	109 217	1.3762	−1313
$5s^25p^45d$	[0]	1/2	105 948	1.36	107 566	1.1311	−1618
$5s^25p^46p$	[2]°	3/2	111 792	1.61	112 248	1.6084	−456
		5/2	111 959	1.47	112 286	1.4934	−327
$5s^25p^46p$	[3]°	5/2	113 512	1.28	114 041	1.2350	−529
		7/2	113 705	1.40	114 266	1.3984	−561
$5s^25p^46p$	[1]°	1/2	113 673	1.50	114 350	1.5358	−677
		3/2	116 783	1.37	117 621	1.3609	−838

[a] $\Delta = E(\text{expt}) - E(\text{calc})$.

$5s^25p^55d$ configuration. The detailed study of the ways to saturate the basis goes beyond the scope of the present work.

Apart from numerical accuracy comparison of the theory and experiment can be affected by omitting of the higher-order relativistic effects from the atomic Hamiltonian. In the present paper we do not include Breit interaction and quantum electrodynamic (QED) corrections. The study of Breit interaction in many-electron atoms can be found elsewhere (see, e.g. [30–34]). In particular, the detailed study of the Breit interaction [32,35,36] and QED corrections [37] for cesium, which is next to xenon in the Periodic Table, shows that the effect of these terms on the energy levels is just a small fraction of percent and can be neglected in present calculations.

Tables IV–IX present our results for xenon positive ions from Xe VII to Xe II. Only results obtained in the "best" approximation ($\hat{\Sigma}^{(\infty)}$) are included. Calculations for the ions start from point (4) in the scheme presented in the beginning of this section. This is because the first three points are exactly the same as for neutral xenon. Note that one of the most time consuming steps, calculation of $\hat{\Sigma}_1$, does not need to be repeated. Basis states for valence electrons used in the CI calculations are described in the preceding section (see Table II). We use a shorter basis for the ions because we calculate only lowest states. To go up in the spectrum we would need to extend the basis similar to what is done for Xe I. The analysis of the data in Tables IV–IX show that the accuracy is generally very good in spite of a very short basis.

TABLE X. Energies (cm^{-1}) and g factors of the $5s^25p^58s$ configuration of Xe I.

		Expt. [26]		Calculations	
State	J	E	g	E	g
$8s$ [3/2]°	2	90 805	1.465	92 288	1.5000
	1	90 933	1.182	92 414	1.1700
$8s'$ [1/2]°	0			104 063	0
	1	101 426		104 118	1.3300

For the Xe III ion we also included calculations which use the basis states of the Xe IV ion [column $E(N\text{-}1)$ of Table VIII]. The purpose of these calculations will be explained in the *negative ions* section below.

VII. SOME SPECIAL CASES

A. Highly excited states

One of the additional advantages of the use of V^N basis for valence states is the possibility to study highly excited states with a very short basis. To get to a highly excited state with an universal basis like B-splines one has to calculate all states of the same parity and total momentum J which are below the state of interest. Also, the completeness of the basis deteriorates rapidly while going higher in the spectrum. V^N basis is free from these problems. To calculate highly excited states of a particular configuration it is sufficient to include into single-electron basis for valence states only states which correspond to this configuration. For example, the states of the $5s^25p^58s$ of Xe I can be calculated with good accuracy with only four states in the basis: $5s$, $5p_{1/2}$, $5p_{3/2}$, and $8s$ (see Table X). There are many lower states of same parity and total momentum J but we can easily get rid of them by not including corresponding single-electron states into the basis.

B. Negative ions

An interesting question is whether the method presented in this paper can be used to calculated states of a negative ion. At first glance the answer is *no* because we use V^N states for the basis and negative ions are not bound in the V^N approximation. However, we may consider the following question: What is going to happen if we add one more electron to the CI calculations for a neutral atom, when basis corresponds to the neutral atom?

For atoms like xenon, which do not form negative ions, it makes more sense to consider a more general question: Can a basis calculated for a system of N-1 valence electrons be used to calculate many electron states of a system of N electrons? This can be easily checked. Take, for example, the

Xe IV ion and add one more electron in the CI calculations to get the states of Xe III. We have done this without adding any new states into the basis. Results are presented in the last column of Table VIII. We can see that the results for the ion with the basis of the other ion are almost as good as with its own basis. Accuracy is a bit lower which is a natural consequence of the worsening of the basis. Adding more states to the basis would most certainly improve the results.

This findings are not very surprising since we know that any basis set can be used in the CI calculations. For example, in Ref. [23] calculations for neutral Kr were performed with the basis corresponding to Kr IX The only question is how many states we need to include to get reasonable results. It turns out that at least in the case of just one more electron there is no need to greatly increase the basis. This means that we can also calculate states of negative ions by using basis states of a neutral atom.

VIII. CONCLUSION

In this paper we present a method of calculation for many-electron atoms with open shells which is both accurate and very efficient. The method is based on the so-called V^{N-M} approximation in which calculations start from the highly charged ion with all valence electrons removed. High accuracy is achieved by inclusion of core-valence correlations by means of MBPT. Dominating chains of higher order diagrams are included in all orders. High efficiency of the method is mostly due to the compact V^N basis set for the states of valence electrons. The method is expected to work well for atoms in which valence electrons form a separate shell (defined by the principal quantum number). This is usually the case if valence electrons in the atomic ground state occupy s and/or p states. This covers roughly half of the Periodic Table of elements. Calculations for xenon and its ions illustrate the use of the method.

ACKNOWLEDGMENTS

The authors are grateful to W. R. Johnson and M. G. Kozlov for useful discussions. The work was funded in part by the Australian Research Council.

APPENDIX: EFFICIENT WAY OF CALCULATING $\hat{\Sigma}$

The correlation correction operator $\hat{\Sigma}_1$ is defined in such are way that its average value over a wave function of a valence electron is the correlation correction to the energy of this electron:

$$\delta\epsilon_v = \langle v|\hat{\Sigma}_1|v\rangle. \tag{A1}$$

We use the following form of the single-electron wave function:

$$\psi(r)_{njlm} = \frac{1}{r}\begin{pmatrix} f_n(r)\Omega(\mathbf{n})_{jlm} \\ i\alpha g_n(r)\tilde{\Omega}(\mathbf{n})_{jlm} \end{pmatrix}. \tag{A2}$$

Then the expression (A1) becomes

$$\begin{aligned}\delta\epsilon_v = &\int\int f_v(r)\Sigma_{ff}(r,r')f_v(r')dr\,dr' \\ &+ \alpha^2\int\int f_v(r)\Sigma_{fg}(r,r')g_v(r')dr\,dr' \\ &+ \alpha^2\int\int g_v(r)\Sigma_{gf}(r,r')f_v(r')dr\,dr' \\ &+ \alpha^4\int\int g_v(r)\Sigma_{gg}(r,r')g_v(r')dr\,dr'. \end{aligned}\tag{A3}$$

Note factors α^2 and α^4 in all terms except the first one. These factors make corresponding contributions very small. Therefore, we do not usually include them. Only Σ_{ff} will be considered in this appendix and we will omit the indexes.

1. Second-order $\hat{\Sigma}$

Good efficiency in calculating of $\hat{\Sigma}$ is achieved by dividing the calculations into two steps.

(1) First, all relevant Coulomb Y functions are calculated and stored on disk.

(2) Then, Σ is calculated using stored Y functions.

The Coulomb Y function is defined as

$$Y_{knm}(r) = \int \frac{r_<^k}{r_>^{k+1}}[f_n(r')f_m(r') + \alpha^2 g_n(r')g_m(r')]dr', \tag{A4}$$

where $r_<=\min(r,r')$ and $r_>=\max(r,r')$. We will also need a ρ function:

$$\rho_{jl}(r) = f_j(r)f_l(r) + \alpha^2 g_j(r)g_l(r). \tag{A5}$$

Our typical coordinate grid consists of about 1000 points. Usually all of them are used to calculate Y functions (A4). However, there is no need to keep all points for the Y and ρ functions for consequent calculations. It turns out that very little loss of accuracy is caused by the use of a subset of points defined as every fourth point in the interval

$$1/Z \leqslant r \leqslant R_{\text{core}}.$$

By cutting off the point on short and large distances and using only every fourth point in between we reduce the number of points by an order of magnitude. Then, Coulomb integrals are calculated in an extremely efficient way

$$q_k(jlmn) = \sum_{i=1}^{\mu} \rho_{jl}(r_i)Y_{kmn}(r_i)w_i. \tag{A6}$$

Here $\mu \approx 100$ is the number of points on the subgrid and w_i are weight coefficients corresponding to a particular method of numerical integration. Note that only one of two integrations for Coulomb integrals is done on a reduced subgrid. First integration (A4) is done with the use of all points.

An expression for $\hat{\Sigma}_1^{(2)}$ via Y functions is

$$\Sigma_1(r,r') = \sum_{amnk} c_1(kvamn)\frac{f_n(r)Y_{kam}(r)Y_{kam}(r')f_n(r')}{\epsilon_v + \epsilon_a - \epsilon_m - \epsilon_n} \tag{A7}$$

$$- \sum_{amnk_1k_2} c_2(k_1k_2vamn) \times \frac{f_n(r)Y_{k_1am}(r)Y_{k_2an}(r')f_m(r')}{\epsilon_v + \epsilon_a - \epsilon_m - \epsilon_n} \tag{A8}$$

$$- \sum_{amnk} c_3(kvabm) \frac{f_b(r)Y_{kam}(r)Y_{kam}(r')f_b(r')}{\epsilon_a + \epsilon_b - \epsilon_v - \epsilon_m} \tag{A9}$$

$$+ \sum_{amnk_1k_2} c_4(k_1k_2vabm) \times \frac{f_a(r)Y_{k_1bm}(r)Y_{k_2am}(r')f_b(r')}{\epsilon_a + \epsilon_b - \epsilon_v - \epsilon_m}. \tag{A10}$$

Here c_1, c_2, c_3, c_4 are angular coefficients. Expressions for them can be found elsewhere [16]. Formulas (A7)–(A10) correspond to diagrams 1, 2, 3, and 4 on Fig. 2. $\hat{\Sigma}_1$ is a matrix of size $\mu \approx 100$ in coordinate space. Matrix elements of $\hat{\Sigma}_1$ are calculated by

$$\langle v|\hat{\Sigma}_1|w\rangle = \sum_{i=1,j=1}^{\mu} f_v(r_i)\Sigma_1(r_i,r_j)f_w(r_j)w_iw_j. \tag{A11}$$

Note that we use a two-step procedure to calculate matrix elements of $\hat{\Sigma}_1$. First, $\hat{\Sigma}_1$ matrix which is independent on valence functions is calculated, then matrix elements of $\hat{\Sigma}_1$ are calculated. To use the same approach for $\hat{\Sigma}_2$ is impractical. As can be seen from Fig. 4 to make $\hat{\Sigma}_2$ independent on valence states one would have to make matrices of dimensions 2, 3, and 4. Therefore, we just calculate matrix elements of $\hat{\Sigma}_2$ via Coulomb integrals. Corresponding expressions can be found in Ref. [16]. Coulomb integrals are calculated as in Eq. (A6).

2. All-order Σ

We use the Feynman diagram technique to include higher-order correlations into the direct part of $\hat{\Sigma}_1$ (diagrams 1 and 3 on Fig. 2). The corresponding expression is [9]

$$\Sigma(\epsilon, r_i, r_j) = \sum_{nm} \int \frac{d\omega}{2\pi} G_{ij}(\epsilon + \omega) Q_{im} \tilde{\Pi}_{mn}(\omega) Q_{nj}. \tag{A12}$$

Here $\tilde{\Pi}$ is "screened polarization operator"

$$\tilde{\Pi} = \Pi[1 - Q\Pi]^{-1},$$

Π is polarization operator

$$\Pi(\omega) = \sum_a \psi_a[G(\epsilon_a + \omega) + G(\epsilon_a - \omega)]\psi_a,$$

G is Green function

$$(\hat{h}_1 - \epsilon)G(r,r') = -\delta(r - r'),$$

and Q is Coulomb interaction

$$Q_{ij} = e^2/(r_i - r_j).$$

The details of calculation of $\hat{\Sigma}_1^{(\infty)}$ can be found elsewhere [7,9]. Here we only want to mention that operators $\tilde{\Pi}$, Π, G, and Q are matrices of size $\mu \approx 100$ in coordinate space. Therefore, calculation of $\hat{\Sigma}_1^{(\infty)}$ involves manipulation of matrices of relatively small size. If we also recall that $\hat{\Sigma}_1$ does not depend on valence states and needs to be calculated only once then the efficiency of its calculation is quiet satisfactory.

Higher-order correlations in exchange diagrams for $\hat{\Sigma}_1$ (diagrams 2 and 4 on Fig. 2) and for all diagrams for $\hat{\Sigma}_2$ are included via screening factors as explained in the text.

[1] J. S. M. Ginges and V. V. Flambaum, Phys. Rep. **397**, 63 (2004).

[2] J. K. Webb, V. V. Flambaum, C. W. Churchill, M. J. Drinkwater, and J. D. Barrow, Phys. Rev. Lett. **82**, 884 (1999); J. K. Webb, M. T. Murphy, V. V. Flambaum, V. A. Dzuba, J. D. Barrow, C. W. Churchill, J. X. Prochaska, and A. M. Wolfe, *ibid.* **87**, 091301 (2001); M. T. Murphy, J. K. Webb, V. V. Flambaum, V. A. Dzuba, C. W. Churchill, J. X. Prochaska, J. D. Barrow, and A. M. Wolfe, Mon. Not. R. Astron. Soc. **327**, 1208 (2001).

[3] E. J. Angstmann, V. A. Dzuba, and V. V. Flambaum, Phys. Rev. A **70**, 014102 (2004); J. Angstmann, V. A. Dzuba, V. V. Flambaum, A. Yu. Nevsky, and S. G. Karshenboim, J. Phys. B **39**, 1937 (2006).

[4] K. Beloy, U. I. Safronova, and A. Derevianko, Phys. Rev. Lett. **97**, 040801 (2006); E. J. Angstmann, V. A. Dzuba, and V. V. Flambaum, *ibid.* **97**, 040802 (2006); Phys. Rev. A **74**, 023405 (2006).

[5] A. Landau, E. Eliav, Y. Ishikawa, and U. Kaldor, J. Chem. Phys. **114**, 2977 (2001); E. Eliav, A. Landau, Y. Ishikawa, and U. Kaldor, J. Phys. B **35**, 1693 (2002).

[6] V. A. Dzuba, V. V. Flambaum, P. G. Silvestrov, and O. P. Sushkov, J. Phys. B **20**, 1399 (1987).

[7] V. A. Dzuba, V. V. Flambaum, and O. P. Sushkov, Phys. Lett. A **140**, 493 (1989); Phys. Lett. A **141**, 147 (1989); V. A. Dzuba, V. V. Flambaum, A. Ya. Kraftmakher, and O. P. Sushkov, *ibid.* **142**, 373 (1989).

[8] S. A. Blundell, W. R. Johnson, and J. Sapirstein, Phys. Rev. Lett. **65**, 1411 (1990); S. A. Blundell, J. Sapirstein, and W. R. Johnson, Phys. Rev. D **45**, 1602 (1992).

[9] V. A. Dzuba, V. V. Flambaum, and J. S. M. Ginges, Phys. Rev. D **66**, 076013 (2002).

[10] V. A. Dzuba, V. V. Flambaum, P. G. Silvestrov, and O. P. Sushkov, J. Phys. B **20**, 3297 (1987).

[11] M. G. Kozlov, S. G. Porsev, and W. R. Johnson, Phys. Rev. A **64**, 052107 (2001).
[12] Hsiang-Shun Chou and W. R. Johnson, Phys. Rev. A **56**, 2424 (1997); S. A. Blundell, W. R. Johnson, and J. Sapirstein, *ibid.* **42**, 3751 (1990).
[13] S. A. Blundell, W. R. Johnson, and J. Sapirstein, Phys. Rev. A **43**, 3407 (1991); A. Landau, E. Eliav, Y. Ishikawa, and U. Kaldor, J. Chem. Phys. **121**, 6634 (2004).
[14] K. T. Cheng, M. H. Chen, W. R. Johnson, and J. Sapirstein, Phys. Rev. A **50**, 247 (1994); K. T. Cheng and M. H. Chen, Radiat. Phys. Chem. **75**, 1753 (2006); P. Bogdanovich, D. Majus, and T. Pakhomova, Phys. Scr. **74**, 558 (2006).
[15] I. P. Grant, Comput. Phys. Commun. **84**, 59 (1994).
[16] V. A. Dzuba, V. V. Flambaum, and M. G. Kozlov, Phys. Rev. A **54**, 3948 (1996).
[17] V. A. Dzuba and W. R. Johnson, Phys. Rev. A **57**, 2459 (1998).
[18] V. A. Dzuba, V. V. Flambaum, M. G. Kozlov, and S. G. Porsev, JETP **87**, 885 (1998).
[19] I. M. Savukov and W. R. Johnson, Phys. Rev. A **65**, 042503 (2002).
[20] I. M. Savukov, W. R. Johnson, and H. G. Berry, Phys. Rev. A **66**, 052501 (2002).
[21] I. M. Savukov, J. Phys. B **36**, 2001 (2003).
[22] V. A. Dzuba and J. S. M. Ginges, Phys. Rev. A **73**, 032503 (2006); V. A. Dzuba and V. V. Flambaum, J. Phys. B **40**, 227 (2007).
[23] V. A. Dzuba, Phys. Rev. A **71**, 032512 (2005).
[24] V. A. Dzuba and V. V. Flambaum, Phys. Rev. A **71**, 052509 (2005).
[25] V. A. Dzuba, Phys. Rev. A **71**, 062501 (2005).
[26] NIST Atomic Spectra Database on Internet, http://physics.nist.gov/cgi-bin/AtData/main_asd.
[27] J. L. Heully, I. Lindgren, E. Lindroth, and A. M. Mårtensson-Pendrill, Phys. Rev. A **33**, 4426 (1986); A.-M. Mårtensson-Pendrill, I. Lindgren, E. Lindroth, S. Salomonson, and D. S. Staudte, *ibid.* **51**, 3630 (1995).
[28] W. R. Johnson, *Atomic Structure Theory: Lectures on Atomic Physics* (Springer-Verlag, Berlin, 2007).
[29] P. Indelicato, Phys. Rev. A **51**, 1132 (1995).
[30] E. Lindroth, A. M. Mårtensson-Pendrill, A. Ynnerman, and P. Öster, J. Phys. B **22**, 2447 (1989).
[31] E. Lindroth and A. Ynnerman, Phys. Rev. A **47**, 961 (1993).
[32] A. Derevianko, Phys. Rev. A **65**, 012106 (2002).
[33] P. Indelicato, A. M. Mårtensson-Pendrill, W. Quint, and J. P. Desclaux, Hyperfine Interact. **146-147**, 127 (2003).
[34] G. Tommaseo, T. Pfeil, G. Revalde, G. Werth, P. Indelicato, and J. P. Desclaux, Eur. Phys. J. D **25**, 113 (2003).
[35] V. A. Dzuba, C. Harabati, W. R. Johnson, and M. S. Safronova, Phys. Rev. A **63**, 044103 (2001).
[36] V. A. Dzuba, V. V. Flambaum, and M. S. Safronova, Phys. Rev. A **73**, 022112 (2006).
[37] V. V. Flambaum and J. S. M. Ginges, Phys. Rev. A **72**, 052115 (2005).